Design and expected performance of the MICE Demonstration of Ionization Cooling

The MICE collaboration

Muon beams of low emittance provide the basis for the intense, well-characterised neutrino beams necessary to elucidate the physics of flavour at a neutrino factory and to provide lepton-antilepton collisions at energies of up to several TeV at a muon collider. The International Muon Ionization Cooling Experiment (MICE) aims to demonstrate ionization cooling, the technique by which it is proposed to reduce the phase-space volume occupied by the muon beam at such facilities. In an ionization-cooling channel, the muon beam passes through a material (the absorber) in which it loses energy. The energy lost is then replaced using RF cavities. The combined effect of energy loss and re-acceleration is to reduce the transverse emittance of the beam (transverse cooling). A major revision of the scope of the project was carried out over the summer of 2014. The revised project plan can deliver a demonstration of ionization cooling. The design of the cooling demonstration experiment will be described together with the cooling performance of the revised configuration.

1 Introduction

Stored muon beams have been proposed as the source of neutrinos at a neutrino factory and as the means to deliver multi-TeV lepton-antilepton collisions at a muon collider [1]. In such facilities the muon beam is produced from the decay of pions produced by a high-power proton beam striking a target. The tertiary muon beam occupies a large volume in phase space. To optimise the muon yield while maintaining a suitably small aperture in the muon-acceleration systems requires that the muon-beam phase space be reduced (cooled) prior to acceleration. The short particle lifetime makes traditional cooling techniques unacceptably inefficient when applied to muon beams. Ionization cooling, in which the muon beam is passed through material (the absorber) and subsequently accelerated, is the technique by which it is proposed to cool the beam [2, 3]. This technique has never been demonstrated experimentally, and such a demonstration is believed to be essential to the development of future high-brightness muon accelerators.

The MICE collaboration proposes a two-part process by which to perform a full demonstration of transverse ionization cooling. First, the "Step IV" configuration will be used to study of the properties that determine the performance of an ionization-cooling lattice. Secondly, a study of transverse-emittance reduction in a cooling cell that includes accelerating cavities will be performed.

The cooling performance of an ionization-cooling cell depends on the emittance and momentum of the initial beam, on the properties of the absorber material and on the transverse betatron function ($\beta_\perp$) at the absorber. These factors will be studied using the Step IV configuration [4]. At this stage the muon beam, focused by superconducting solenoids, interacts with the absorber (either liquid hydrogen or lithium hydride), however no acceleration is performed at Step IV. Once the properties of the absorber material, the inital beam parameters and the lattice optics, have been characterised fully at Step IV, "sustainable" ionization cooling must be demonstrated. This requires restoring energy lost by the muons as they pass through the absorber using RF cavities. The experimental configuration with which the MICE collaboration originally proposed to study ionization cooling was presented in [5]. This proposed configuration has been revised in the light of the recommendations of national and international reviews of the project. This paper describes the lattice configuration proposed by the MICE collaboration for the demonstration of ionization cooling and presents prediction of its performance.

2 Cooling in neutrino factories and in muon colliders

Muons are produced occupying a large area of phase space (i.e. large emittance), which must be condensed before acceleration. In the case of a neutrino factory [6] the transverse emittance must be reduced from 15–20 mm to 2–5 mm. A muon collider [1] requires even further cooling to have a sufficient luminosity ($\approx 10^{34}$ cm^{-2}s^{-1}), reducing the emittance to 0.4 mm in the transverse plane, and 1 mm in the longitudinal plane.

Synchrotron radiation and stochastic cooling techniques are unsuitable for muon beams due to the short muon lifetime. ionization cooling is the only process that can efficiently reduce the emittance of a muon beam within its lifetime. A beam is passed through a low-Z material (absorber), losing energy by ionization, reducing the phase-space area it occupies. This is sustainable if the beam is re-accelerated, restoring the energy lost in the absorbers. The rate of change of transverse (2D) normalised emittance, ε_N, is given by,

$$\frac{\mathrm{d}\varepsilon_N}{\mathrm{d}s} \backsimeq \frac{\varepsilon_N}{\beta^2 E_\mu}\left\langle\frac{\mathrm{d}E}{\mathrm{d}s}\right\rangle + \frac{\beta_\perp (13.6\ \mathrm{MeV/c})^2}{2\beta^3 E_\mu m_\mu X_0}, \tag{1}$$

where $\beta = \frac{v}{c}$ is the normalised relativistic velocity, E_μ the energy, $\frac{\mathrm{d}E}{\mathrm{d}s}$ the energy loss rate due to ionization, m_μ the mass of the muon, X_0 the radiation length of the absorber and $\beta_\perp$ the transverse betatron function at the absorber [3]. The first term of this equation describes cooling by ionization energy loss, and the second term describes heating by multiple Coulomb scattering.

In order to have good performance in the cooling channel $\beta_\perp$ needs to be minimised and $X_0\langle\frac{\mathrm{d}E}{\mathrm{d}s}\rangle$ maximised. The betatron function at the absorber is most effectively minimised by using a solenoidal focussing channel, and $X_0\langle\frac{\mathrm{d}E}{\mathrm{d}s}\rangle$ is maximised by using a low-Z absorber such as liquid hydrogen (LH_2) or lithium hydride (LiH) [7].

3 The Muon ionization Cooling Experiment

The muons for MICE come from the decay of pions produced at an internal target dipping directly into the circulating proton beam in the ISIS synchrotron at the Rutherford Appleton Laboratory (RAL). A beam line of 9 quadrupoles, 2 dipoles and a superconducting decay solenoid collects and transports the momentum-selected beam into the cooling channel while performing Particle Identification and time-of-flight measurement. A diffuser is installed at the beginning of the cooling channel to vary the initial emittance of the entrance beam. ionization cooling depends on momentum, as shown in Equation 1, so it is proposed that the channel performance is measured in the range of 140–240 MeV/c [1].

3.1 The MICE demonstration cooling channel

The configuration that is proposed to be used for the demonstration of ionization cooling is shown in Fig. 1. It contains two, single 201.25 MHz cavities, one primary (65 mm) LiH absorber, and two secondary (32.5 mm) LiH secondary ("screening") absorbers. The central lithium-hydride (LiH) absorber is sandwiched between two superconducting focus-coil (FC) modules. The emittance is measured upstream and downstream of the cooling channel using solenoidal spectrometers. Further instrumentation upstream and downstream of the magnetic channel serves to select a pure sample of muons passing through the channel and to measure the phase at which each muon passes through the RF cavities. The spectrometer solenoids (SSs) house high-precision scintillating-fibre tracking detectors (trackers) [8] in a uniform field of 4 T. This uniform field is created by three superconducting solenoids (E1, EC, E2), and two matching superconducting coils (M1, M2) are used to adjust the optics between the uniform field region into the FCs. The trackers will be used to reconstruct the trajectories of individual muons at the entrance and exit of the cooling channel. The reconstructed tracks will be

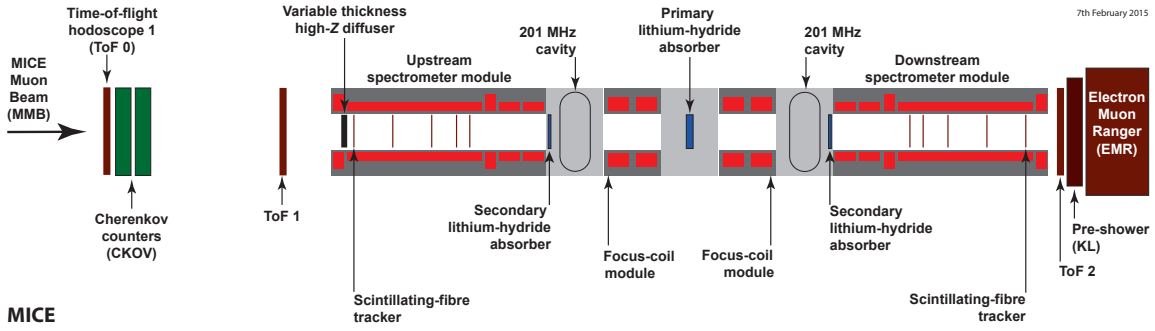

Figure 1: Layout of the lattice configuration for the MICE Cooling Demonstration (DEMO lattice).

combined with the information from the instrumentation upstream and downstream of the channel to measure the muon beam emittance at the tracker reference planes upstream and downstream with a precision of 0.1%.

The secondary LiH absorbers (SAs) are introduced between the cavities and trackers in order to minimise the exposure of the trackers to dark-current electrons originating from the RF cavities. Such electrons produce background to the muon tracks in the trackers. The MuCool Test Area (MTA) has observed that the rate of X-rays from a single MICE RF cavity is not sufficient to damage the SciFi trackers [9]. However, it is still desirable to screen the trackers from the RF cavities. The SAs also increase the net transverse cooling effect. The positions for the SAs were carefully selected as a compromise between the requirement of a small value of beta at absorbers and the ability to remove the absorbers remotely to allow studies of the bare magnetic lattice.

Retractable, lead radiation shutters will be installed on rails between SSs and the RF modules to protect the trackers against dark-current induced radiation during cavity conditioning. The SAs will be mounted on a rail system similar to that which will be used for lead shutters and will be located between the cavities and the lead shutters. Both mechanisms will be moved using linear Piezo-electric motors that operate in vacuum and magnetic field. The design of both the radiation shutter and the movable SA inside the vacuum chamber is shown in Fig. 2.

The RF cavities are sophisticated 201.25 MHz 'pillbox' resonators, 430 mm in length operating in the $TM_{0,1,0}$ mode with large diameter particle beam apertures to accommodate the high emittance beam. The apertures are covered by thin Beryllium windows to define the limits for the accelerating RF fields whilst ensuring minimal scattering of the muons. The cavity is excited by two magnetic loop couplers on opposite sides of the cylindrical waist. At the particle rate expected in MICE there is no loading of the RF fields. The intrinsic quality factor is 5×10^5, whilst the shunt impedance was estimated to be 5.92 MΩ. The peak gap voltage in the proposed configuration is 4.37 MV, or a field of 10.3 MV/m. This estimate was used to define the gradient in the simulations presented in the present paper. Bellows around each cavity module have been added in order to allow easy cavity module inspection.

4 Lattice design

4.1 Design parameters

The lattice has been optimised to maximise the reduction in transverse emittance using the primary and secondary LiH absorbers. This is obtained by matching the betatron function to a small value in the central absorber while minimising its maximum values in the FC modules, which helps to reduce the influence of non-linear optics effects. In this configuration, it is also possible to keep a relatively small betatron function at the position of the secondary absorbers whilst maintaining an acceptable beam size at the position of the cavities.

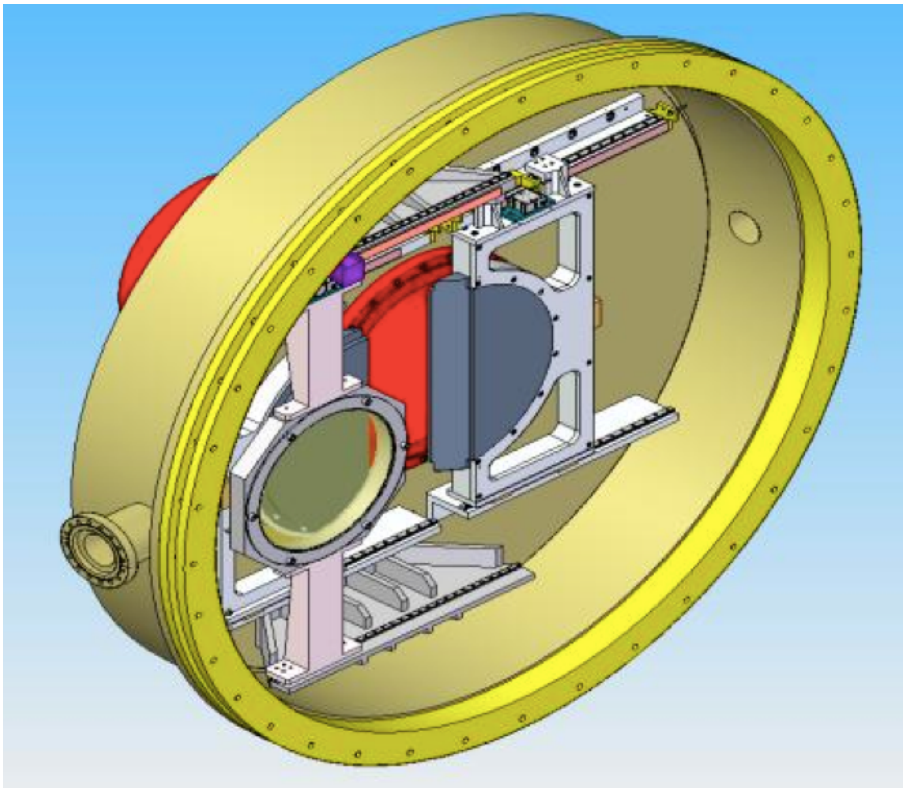

Figure 2: Design of the movable frame for the SA (front) and the lead radiation shutter (back). The half discs of lead shutter (grey) can be seen together with the rails inside the MICE vacuum chamber (yellow).

The phase advance of the cooling cell has been carefully chosen to minimize the chromatic effect due to the large momentum spread of the beam, which leads to a chromatic mismatch in the downstream spectrometer. This reduces the measurable cooling by a chromatic decoherence, which results from a superposition of beam evolutions with different betatron frequencies for different momenta. In addition spherical aberrations resulting from large beam emittance may lead to phase space filamentation. The phase advance of the cell is obtained by integrating the inverse of the beta-function from the reference plane in the SSU to the reference plane in the SSD. The chromatic effects and spherical aberrations were studied with full tracking in order to optimize the cooling effect. The beta-function of the beam with an initial momentum spread of $\pm 4\%$ and emittance evolution for different phase advances are presented in Fig. 3 and Fig. 4, respectively. The phase advance of $2\pi \times 1.81$ shows the best performance for transverse cooling and is thus chosen for the Demonstration of ionization cooling (DEMO) lattice, whose parameters of the lattice are presented in Tab. 1.

Table 1: Design parameters of the DEMO lattice.

Parameter	Value
Length $L_{SS\to FC}$ (mm)	2607.5
Length $L_{FC\to FC}$ (mm)	1678.8
Length $L_{RFmodule\to FC}$ (mm)	784.0
RF Gradient (MV/m)	10.3
Number of RF cavities	2
Number of primary absorbers	1
Number of secondary absorbers	2

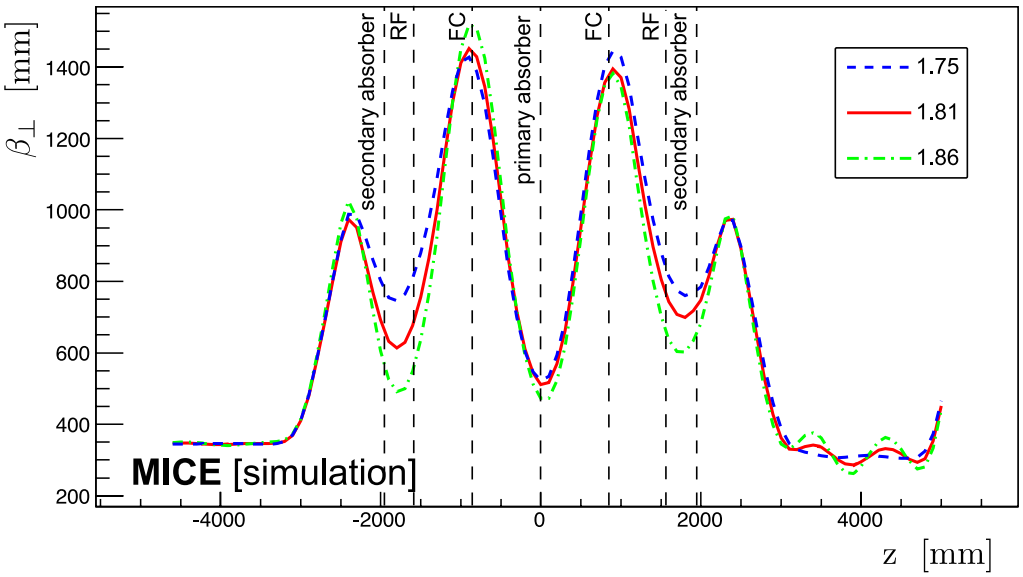

Figure 3: Transverse 4D beta-function in the DEMO lattice for 200 MeV/c settings with a phase advance of $2\pi \times 1.75$ (dashed blue line), $2\pi \times 1.81$ (solid red line) and $2\pi \times 1.86$ (mixed green line).

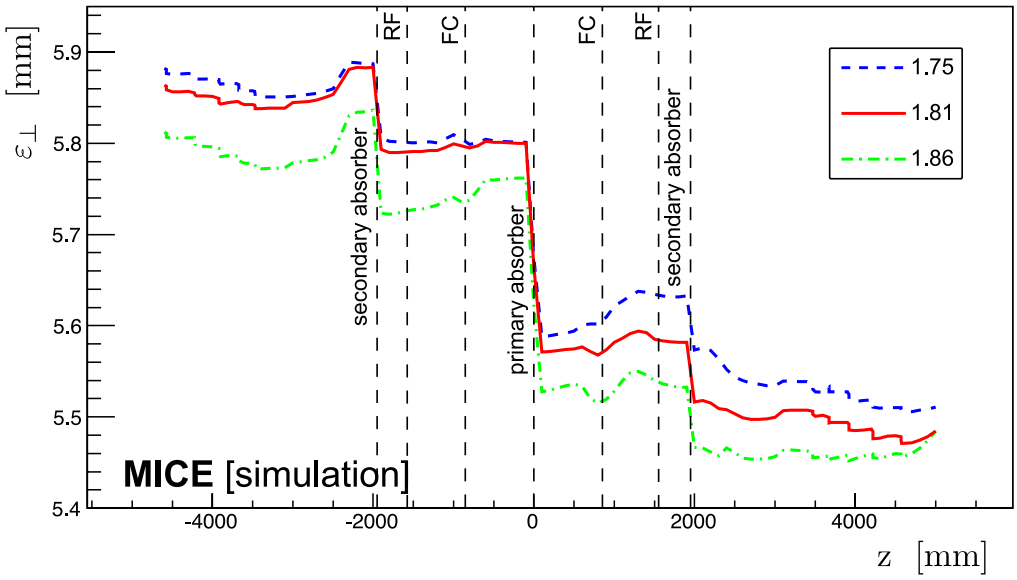

Figure 4: 4D emittance in the DEMO lattice for 200 MeV/c settings with a phase advance of $2\pi \times 1.75$ (dashed blue line), $2\pi \times 1.81$ (solid red line) and $2\pi \times 1.86$ (mixed green line).

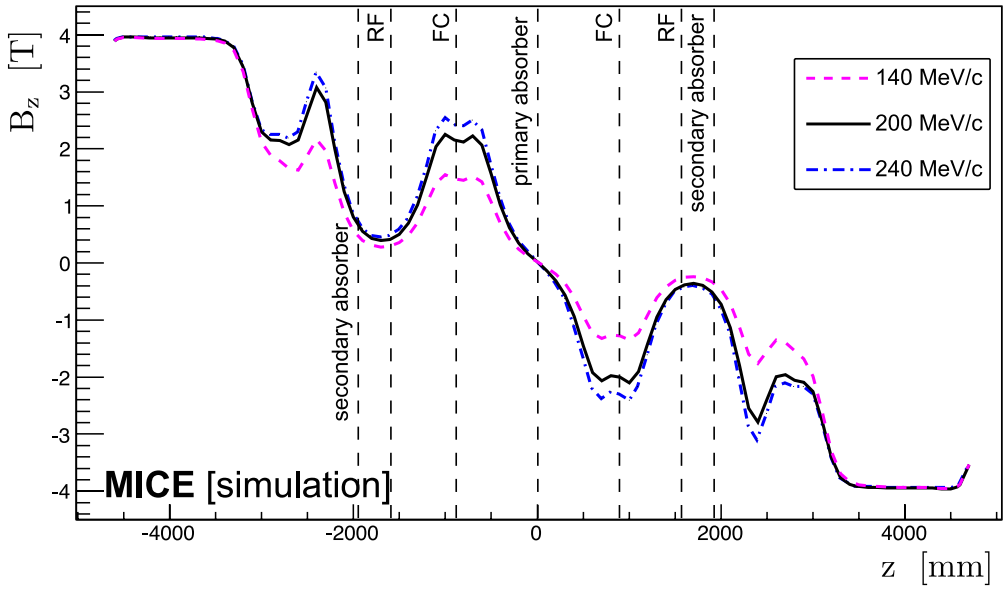

Figure 5: B_z on-axis for the DEMO lattice design for 200 MeV/c (solid black line), for 140 MeV/c (dashed purple line) and for 240 MeV/c (mixed blue line).

The resulting solenoidal magnetic field on axis is shown in Fig. 5 for the three planned settings (140 MeV/c, 200 MeV/c and 240 MeV/c). Vertical lines locate the positions of the centre of the FC modules (red), the primary absorber (burgundy) and the secondary absorbers (blue). This particular configuration powers the downstream FC and SS modules in the opposite sense to the upstream FC and SS so that the field changes sign at the absorber. This is a desirable feature for studying the cancellation of canonical angular momentum through the lattice. Other configurations with different field polarities can also be considered.

Table 2 lists the currents used in this field configuration, all within the proven limits of operation for the individual coil windings. The magnetic forces acting on the coils have been analysed and were found to be acceptable. In particular, the forces experienced by the FC modules are below those expected during Step IV.

The betatron functions shown in Fig. 6 are matched for different initial momentum beams. In all cases, the Courant Snyder parameter $\alpha_\perp = 0$ and the value of the beta-function in each tracker are set for the central momentum to match the constant magnetic field region, and a small beta waist in the central absorber is achieved. This matching takes into account the change in energy of the muons as they pass through the cooling cell by adjusting currents in the upstream and downstream FCs and in the matching coils in the SSs independently while maintaining the field in the tracking volumes at 4 T. Beta values at relevant positions in the different configurations are summarised in Tab. 3.

5 Performance in simulations and reconstruction

5.1 MAUS code

Simulation to evaluate the performance of the lattice have been performed using the official simulation and reconstruction software of MICE called MAUS (MICE Analysis User Software) [10]. In addition to simulation, MAUS also provides a framework for any subsequent data analysis. MAUS is used for both offline analysis and also to provide fast real-time detector reconstruction and data visualization during MICE running.

Table 2: Coil currents used for 140 MeV/c, 200 MeV/c and 240 MeV/c lattice settings.

Coil	140 MeV/c Lattice (A)	200 MeV/c Lattice (A)	240 MeV/c Lattice (A)
Upstream E2	+253.00	+253.00	+253.00
Upstream C	+274.00	+274.00	+274.00
Upstream E1	+234.00	+234.00	+234.00
Upstream M2	+126.48	+155.37	+163.50
Upstream M1	+175.89	+258.42	+280.72
Upstream FC1	+54.14	+79.35	+89.77
Downstream FC1	+54.14	+79.35	+89.77
Upstream FC2	−47.32	−74.10	−85.35
Downstream FC2	−47.32	−74.10	−85.35
Downstream M1	−140.43	−231.60	−261.71
Downstream M2	−100.12	−149.15	−159.21
Downstream E1	−234.00	−234.00	−234.00
Downstream C	−274.00	−274.00	−274.00
Downstream E2	−253.00	−253.00	−253.00

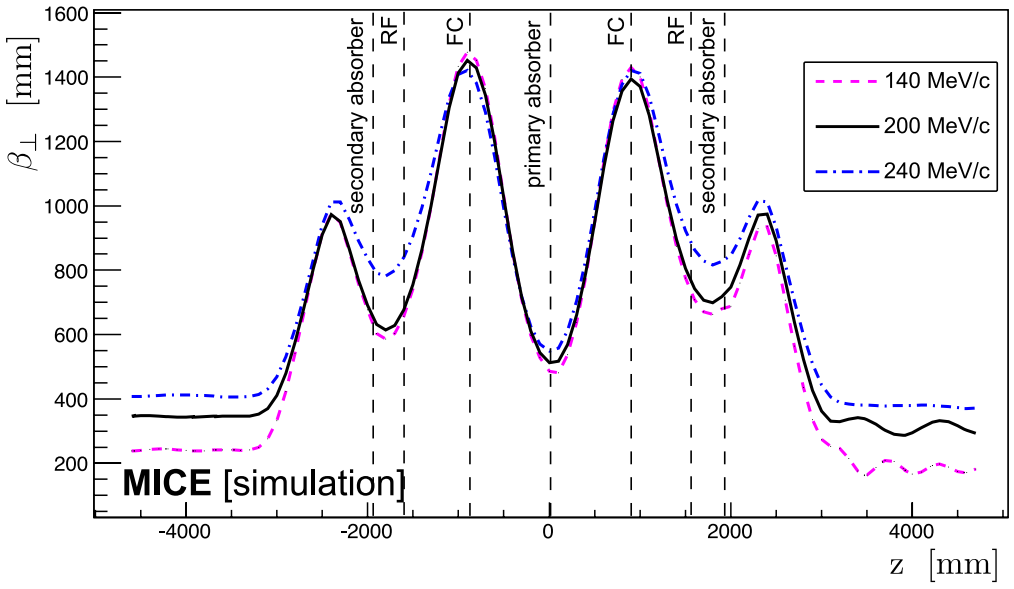

Figure 6: $\beta_\perp$ for 200 MeV/c (solid black line), for 140 MeV/c (dashed purple line) and for 240 MeV/c (mixed blue line) in the DEMO lattice.

Table 3: Beta-function values at relevant positions for an initial beam at 140 MeV/c, 200 MeV/c and 240 MeV/c in the DEMO lattice design.

Parameter	Value for 140 MeV/c	Value for 200 MeV/c	Value for 240 MeV/c
$\beta_\perp$ at primary absorber (mm)	480	512	545
$\beta_\perp$ at secondary absorbers (mm)	660	710	840
$\beta_{\perp\max}$ at FC (mm)	1480	1450	1430

Table 4: General parameters of the initial beam in the different simulations

Parameter	Value
Particle	muon μ^+
Number of particles	10000
Longitudinal position [mm]	-4612.1
Central energy (140 MeV/c conf.) [MeV]	175.4
Central energy (200 MeV/c conf.) [MeV]	228.0
Central energy (240 MeV/c conf.) [MeV]	262.2
Transverses distribution Value Gaussian	
$\alpha_\perp$	0
$\beta_\perp$ (140 MeV/c conf.) [mm]	233.5
$\varepsilon_\perp$ (140 MeV/c conf.) [mm]	4.2
$\beta_\perp$ (200 MeV/c conf.) [mm]	339.0
$\varepsilon_\perp$ (200 MeV/c conf.) [mm]	6.0
$\beta_\perp$ (240 MeV/c conf.) [mm]	400.3
$\varepsilon_\perp$ (240 MeV/c conf.) [mm]	7.2
Longitudinal distribution Value Gaussian	
Longitudinal emittance [mm]	20
Longitudinal β [ns]	11
Longitudinal α	-0.7
rms momentum spread (140 MeV/c conf.)	$\pm$4.8%
rms time spread (140 MeV/c conf.) [ns]	0.40
rms momentum spread (200 MeV/c conf.)	$\pm$4.0%
rms time spread (200 MeV/c conf.) [ns]	0.34
rms momentum spread (240 MeV/c conf.)	$\pm$3.6%
rms time spread (240 MeV/c conf.) [ns]	0.31

GEANT4 is used to support these simulations by providing beam propagation and detector responses, ROOT is used for data visualization and as a data storage format.

5.2 Tracking and analysis

Tracking has been performed for different configurations. Parameters of the initial beam used for the different simulations are summarized in table 4. The beam starts in the simulation after the diffuser and before the first plane of the tracker, and is generated by a randomising algorithm with a fixed seed. Each cavity is simulated by a TM_{010} ideal cylindrical pillbox. The reference particle of the beam is launched to set the phase of the cavities.

The transmission of the lattice represents the proportion of muons that remain after scraping and cuts have been accounted for. Tab. 5 lists the acceptance criteria required by all analyses presented here. Trajectories that fail to meet the acceptance criteria are removed globally.

A muon passing through two 32.5 mm secondary LiH absorbers and one 65 mm primary LiH absorber would lose $\langle \Delta E \rangle = 18.9$ MeV. Including losses in the SciFi trackers and windows, this increases to 24.3 MeV. The RF gradient achievable in two cavities constrained by the available RF drive power (2MW to each cavity) and the requirements to maintain a radiation environment friendly to the scintillating fibre trackers is insufficient to replace the energy lost in the absorber, therefore a comparison of beam energy with and without RF acceleration

Table 5: Acceptance criteria for analysis.

Parameter	Acceptance condition
Particle	muon μ^+
Transmission: pass through two planes	$z = -4600\ mm$ and $z = 5000\ mm$
Radius at $z = -4600\ mm$ (mm)	≤ 150.0
Radius at $z = 5000\ mm$ (mm)	≤ 150.0

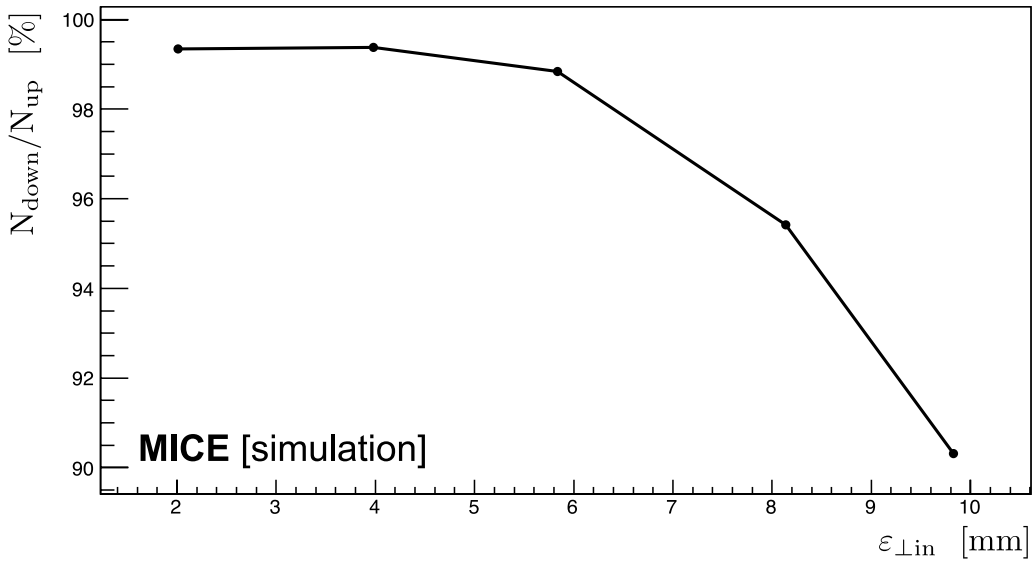

Figure 7: Transmission as a function of initial emittance for the DEMO lattice in the 200 MeV/c configuration.

is required. With RF an energy deficit of $\langle \Delta E \rangle = 19$ MeV would be observed. This measurable difference would confirm that, were more RF cavities or higher RF gradient available, the transverse emittance reduction would be sustainable.

5.3 200 MeV/c configuration performance

The transmission of the lattice in the 200 MeV/c configuration is shown in Figure 7. The maximum theoretical transmission of the DEMO lattice is 99.2%, since muons may decay in the channel. This limits the transmission for low emittances, while the transmission gradually decreases with increasing initial emittance due to scraping.

Figure 8 shows the mean beam energy of an initial $\varepsilon = 6$ mm beam as it crosses the lattice. Energy is lost in the upstream tracker and first secondary absorber before being partially restored in the first RF cavity ($z \approx -1600$ mm). Further energy is lost in the primary absorber, partially restored in the second RF cavity, and then lost in the final secondary absorber.

The reduction in transverse emittance, with RF, is shown in Figure 9. The beam is subject to non-linear effects in regions of high $\beta_\perp$, which causes limited emittance growth. Nonetheless, a reduction in emittance is observed between the upstream and downstream trackers ($z \approx \pm 3500$ mm). The DEMO lattice is predicted to achieve a reduction of ≈ 5.8 %.

Figure 10 shows the fractional change in emittance with respect to the input emittance.

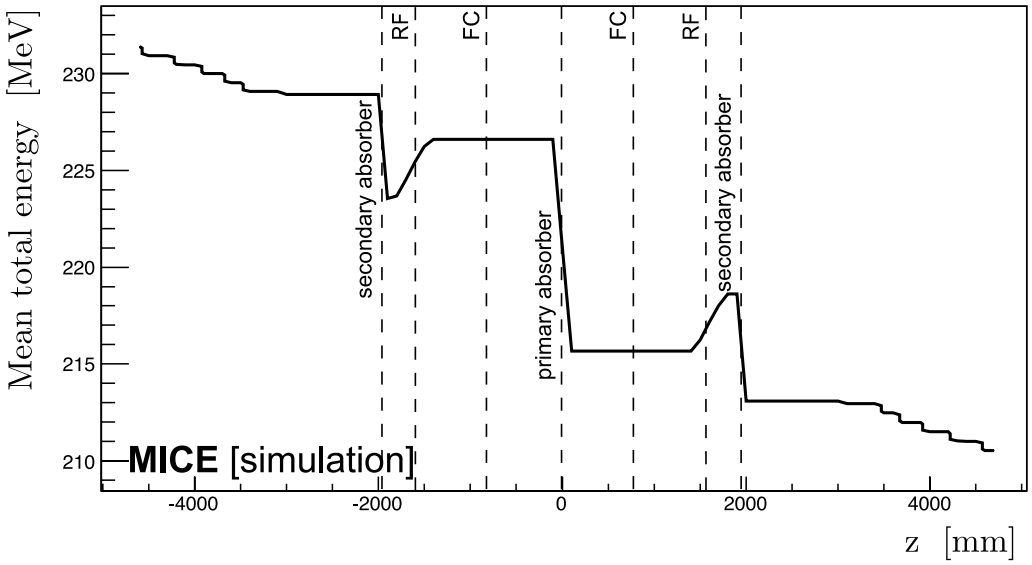

Figure 8: Mean beam energy for the DEMO lattice design in the 200 MeV/c configuration for an initial $\varepsilon = 6$ mm beam.

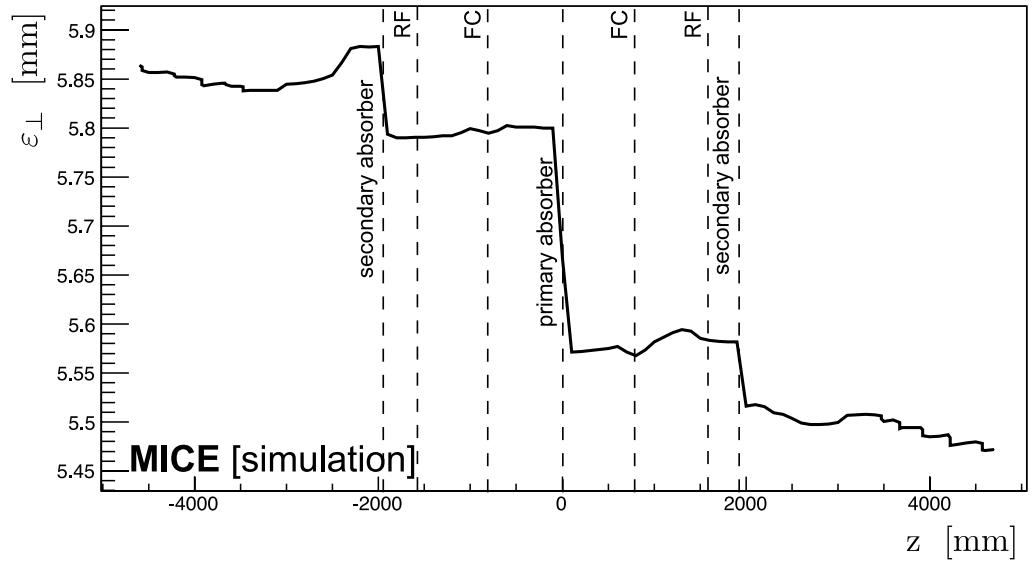

Figure 9: Emittance reduction of an initial $\varepsilon = 6$ mm beam for the DEMO lattice design in the 200 MeV/c configuration.

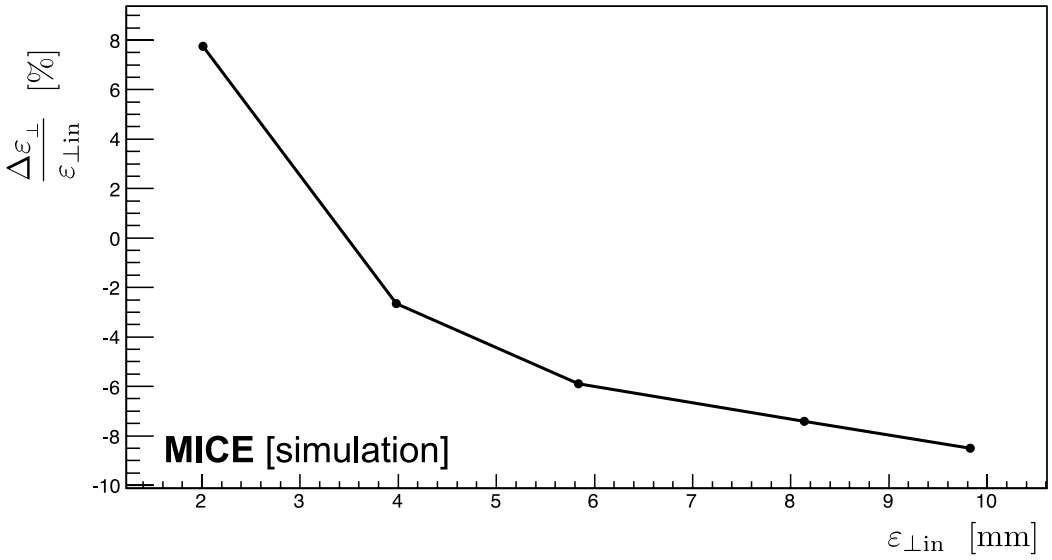

Figure 10: Fractional change in emittance as a function of initial emittance for the DEMO lattice design in the 200 MeV/c configuration.

5.4 140 MeV/c configuration performance

The transmission of the lattice in the 140 MeV/c configuration is shown in Figure 11. In this case, the maximum theoretical transmission of the DEMO lattice is 98.9%, since the energy of the muons is lower.

Figure 12 shows the mean beam energy of an initial $\varepsilon = 4.2$ mm beam as it crosses the lattice. This normalized emittance corresponds to the same geometrical emittance of a $\varepsilon = 6$ mm beam at 200 MeV/c.

The reduction in transverse emittance is shown in Figure 13. The beam is subject to non-linear effects in regions of high $\beta_\perp$, which triggers nonlinear emittance growth in the upstream part and especially in the downstream part. The DEMO lattice is nonetheless predicted to achieve a reduction of ≈ 8.1 %.

These non-linear effects are mainly chromatic effects, since they are greatly lessened when the initial momentum spread is reduced, as presented in Fig. 14, and a ≈ 10 % emittance reduction can be achieved in this case.

Figure 15 shows the fractional change in emittance with respect to the input emittance.

5.5 240 MeV/c configuration performance

The transmission of the lattice in the 240 MeV/c configuration is shown in Figure 16. Here, the maximum theoretical transmission of the DEMO lattice is 99.4%.

Figure 17 shows the mean beam energy of an initial $\varepsilon = 7.2$ mm beam as it crosses the lattice. This normalized emittance corresponds to the same geometrical emittance of a $\varepsilon = 6$ mm beam at 200 MeV/c.

The reduction in transverse emittance, with RF, is shown in Figure 18. The beam is subject to non-linear effects in regions of high $\beta_\perp$, which causes emittance growth. Furthermore, limitations in the maximum currents in the coils prevented the achievement of an optimum focusing. The DEMO lattice is predicted to achieve a reduction of ≈ 4.0 %.

Figure 19 shows the fractional change in emittance with respect to the input emittance.

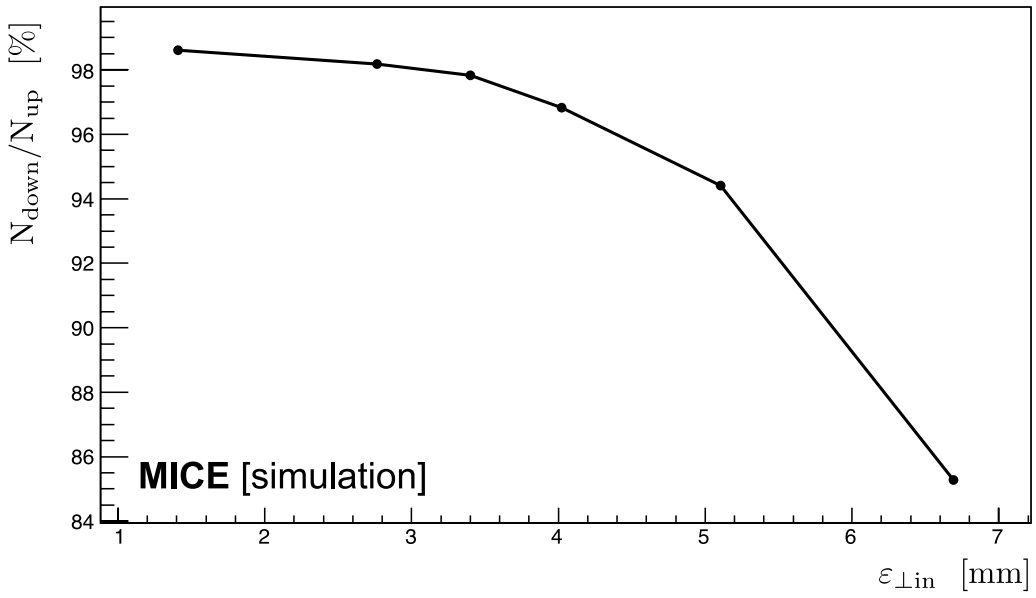

Figure 11: Transmission as a function of initial emittance for the DEMO lattice in the 140 MeV/c configuration.

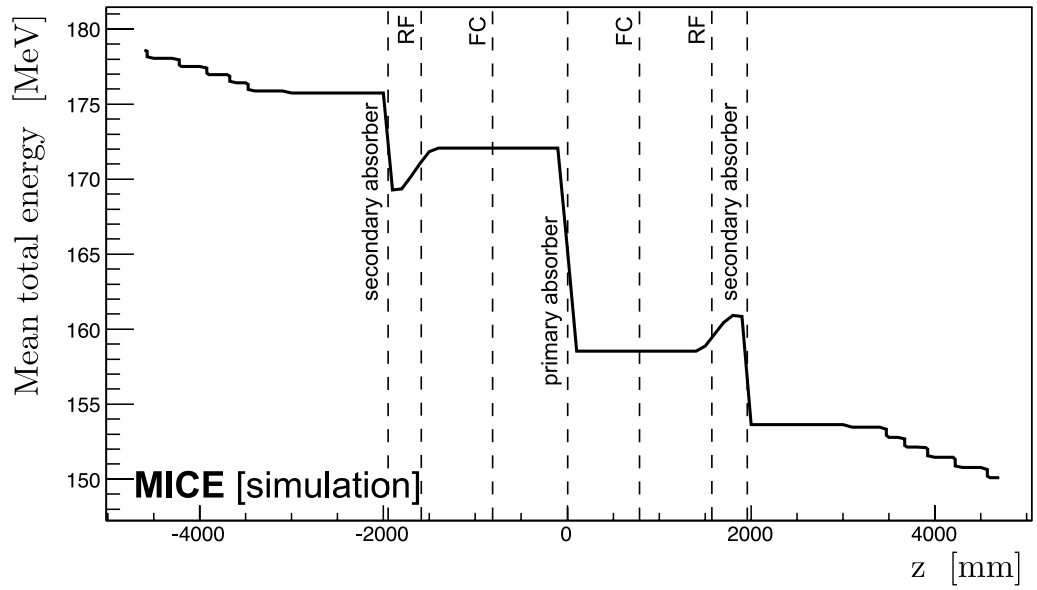

Figure 12: Mean beam energy for the DEMO lattice design in the 140 MeV/c configuration for an initial $\varepsilon = 4.2$ mm beam.

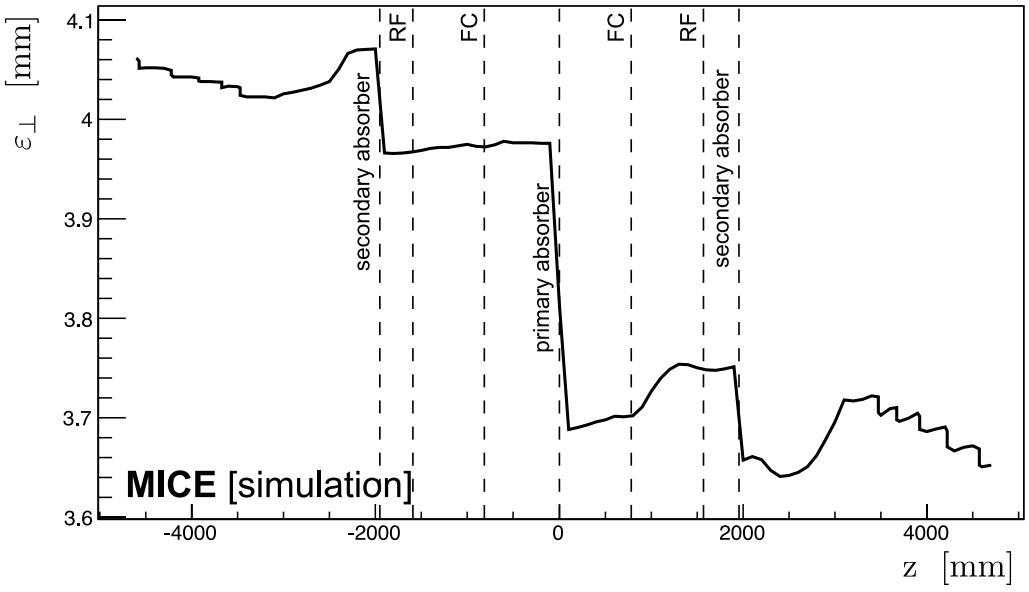

Figure 13: Emittance reduction of an initial $\varepsilon = 4.2$ mm beam with an rms momentum spread of 5.6 MeV/c ($\pm 4\%$) for the DEMO lattice design in the 140 MeV/c configuration.

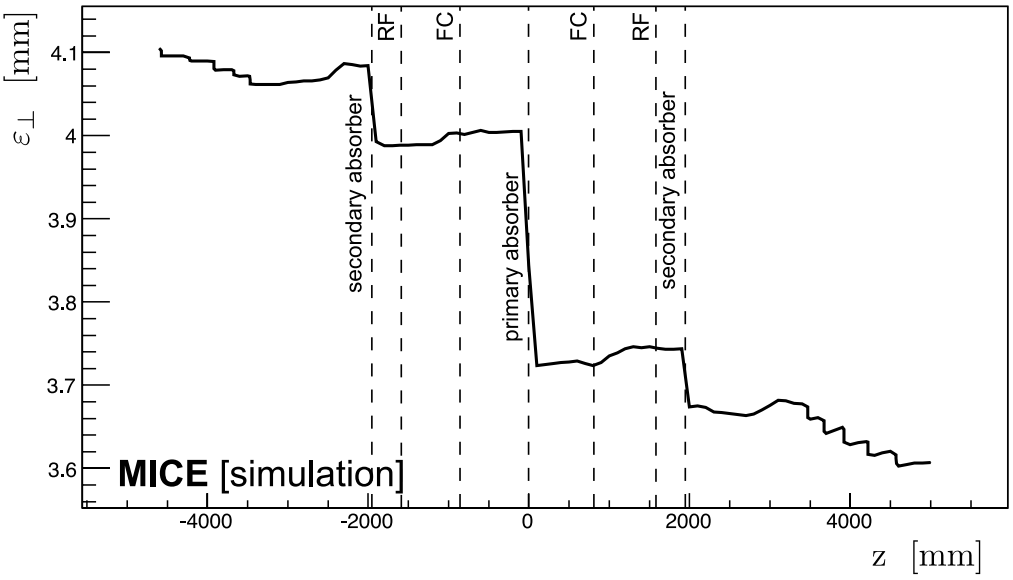

Figure 14: Emittance reduction of an initial $\varepsilon = 4.2$ mm beam with an rms momentum spread of 2.5 MeV/c ($\pm 1.8\%$) for the DEMO lattice design in the 140 MeV/c configuration.

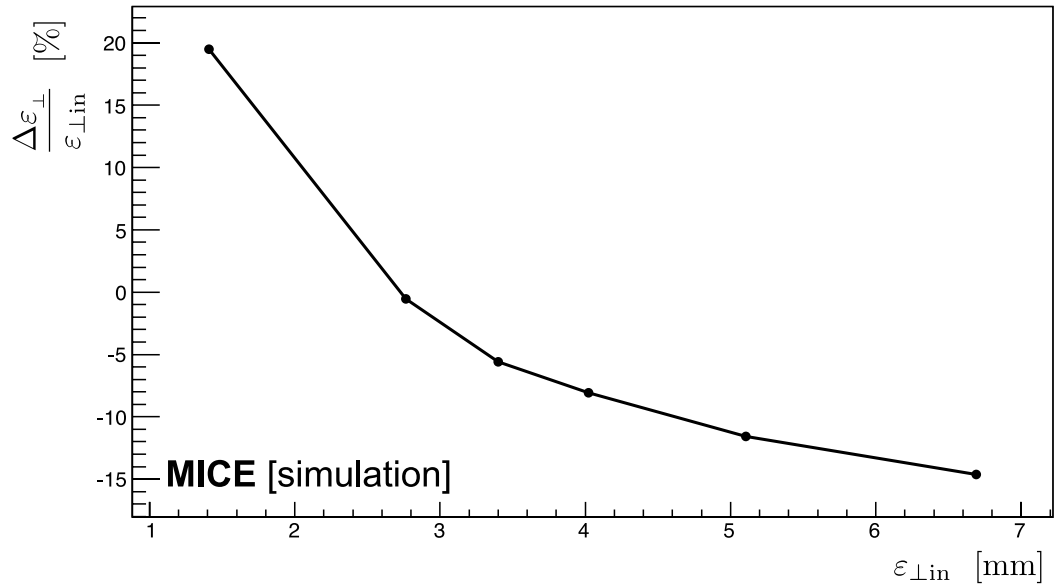

Figure 15: Fractional change in emittance as a function of initial emittance for the DEMO lattice design in the 140 MeV/c configuration.

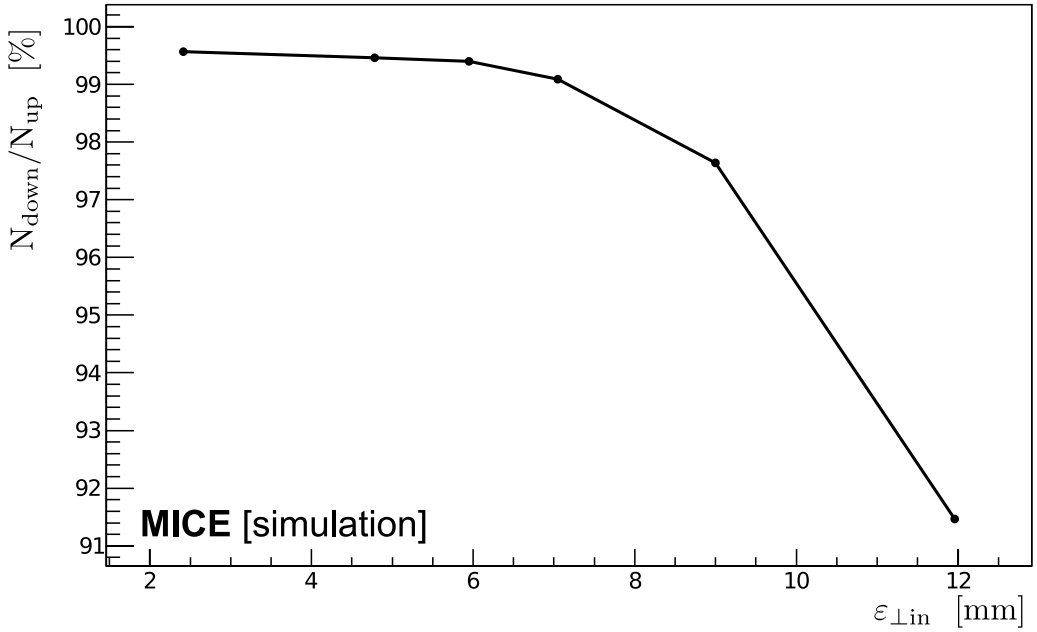

Figure 16: Transmission as a function of initial emittance for the DEMO lattice in the 240 MeV/c configuration.

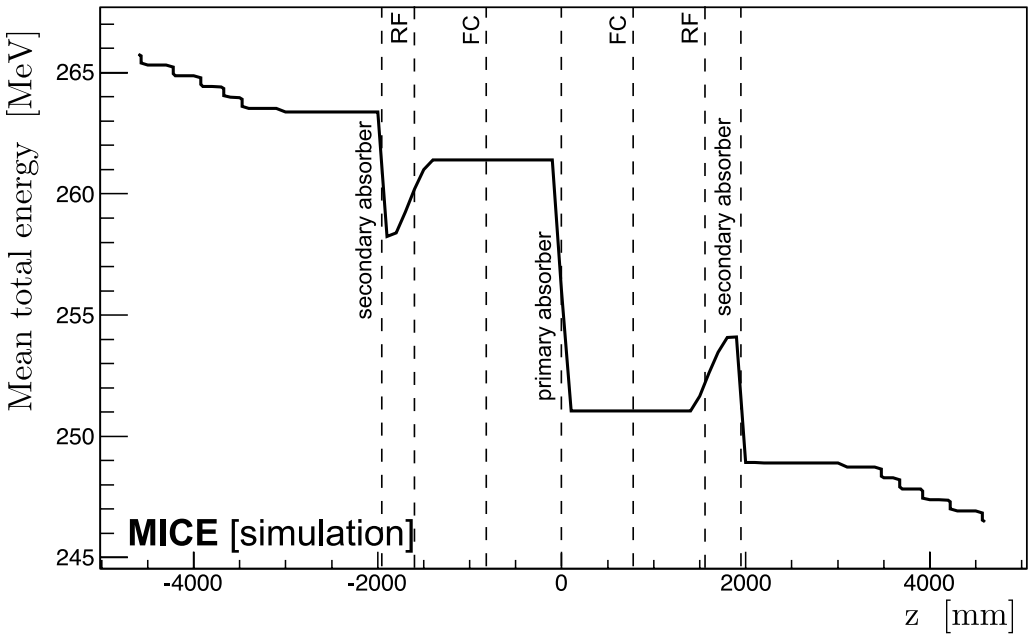

Figure 17: Mean beam energy for the DEMO lattice design in the 240 MeV/c configuration for an initial $\varepsilon = 7.2$ mm beam.

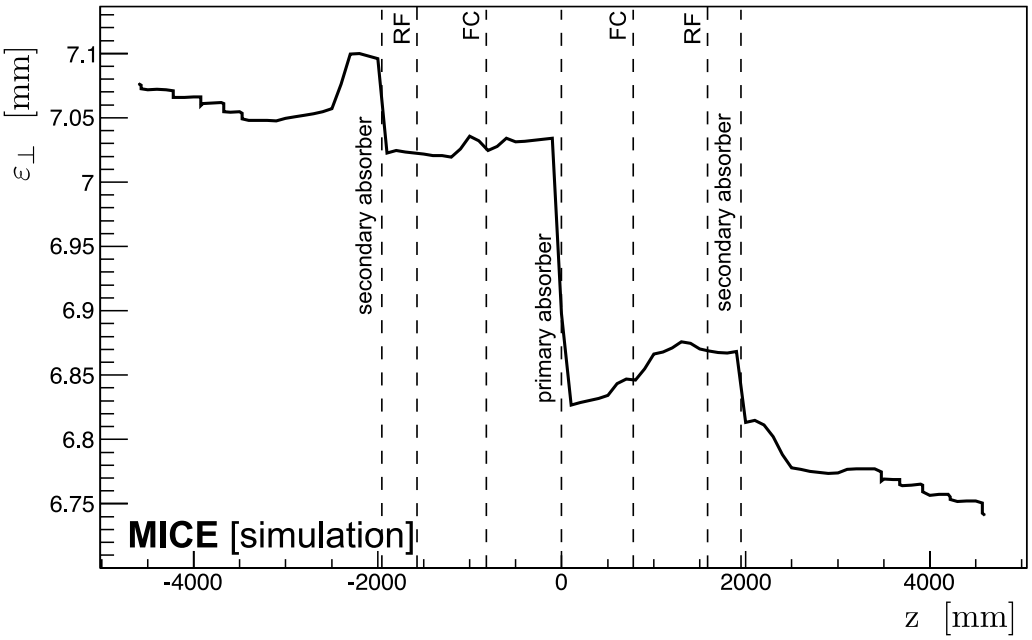

Figure 18: Emittance reduction of a $\varepsilon = 7.2$ mm beam for the DEMO lattice design in the 240 MeV/c configuration.

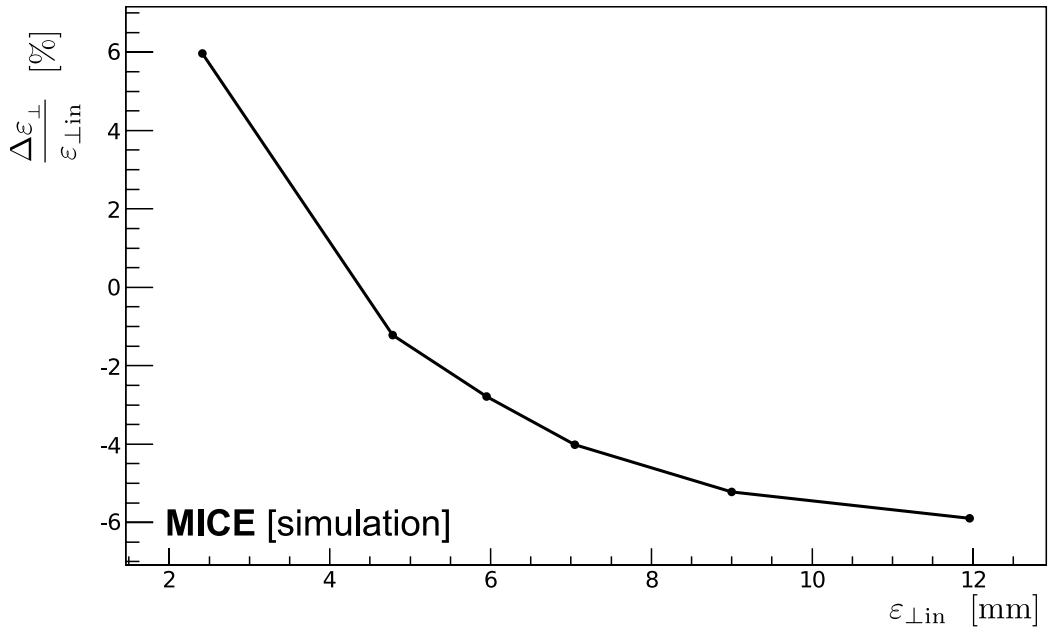

Figure 19: Fractional change in emittance as a function of initial emittance for the DEMO lattice design in the 240 MeV/c configuration.

6 Conclusion

A proposal for the demonstration of ionization cooling has been described that is predicted by simulations to exhibit cooling for several different momenta and optics settings. The demonstration is performed using lithium-hydride absorbers and with acceleration provided by two single, 201.25 MHz, cavity modules. The equipment necessary to mount the experiment is either in hand, like the superconducting magnets and instrumentation, or at an advanced stage of preparation, such as the single-cavity modules. The DEMO configuration has been shown to deliver the performance required for the detailed study of the ionization-cooling technique.

The demonstration of ionization cooling is essential to the future development of muon-based facilities that would provide intense, well characterised muon beams required to elucidate the physics of flavour at a neutrino factory or to deliver multi-TeV lepton-antilepton collisions at a muon collider. The successful completion of the MICE programme would therefore herald the establishment of a new technique for particle physics.

References

[1] S. Geer, "Neutrino beams from muon storage rings: Characteristics and physics potential," *Phys. Rev. D* **57** (1998) 6989–6997.

[2] A. Skrinsky and V. Parkhomchuk, "Cooling methods for beams of charged particles," *Sov. J. Part. Nucl.* **12** (1981) 223.

[3] D. Neuffer, "Principles and applications of muon cooling," *Part. Accel.* **14** (1983) 75.

[4] D. Rajaram et al., "The status of mice step iv," in *Proc. of IPAC2015 Conf.* 2015.

[5] T. M. collaboration, "An international muon ionization cooling experiment (mice)," MICE note 21, Jan., 2003.

[6] The ISS Accelerator Working Group, "Physics at a future neutrino factory and super-beam facility v2," 2007. `http://arxiv.org/abs/0802.4023`. Report number: RAL-TR-2007-23, arXiv:0802.4023v2.

[7] A. Tollestrup and J. Monroe, "Multiple scattering calculations for hydrogen, helium, lithium and beryllium," MuCOOL note 176, 2000.

[8] M. Uchida, "The Alignment of the MICE Tracker Detectors," in *Proc. of IPAC2015 Conf.* 2015.

[9] Y. Torun *et al.*, "Final Commissioning of the MICE RF Module Prototype with Production Couplers," in *Proc. of IPAC2016 Conf.* 2016.

[10] C. D. Tunnell and C. T. Rogers, "MAUS: MICE Analysis User Software," in *Proc. of IPAC2011 Conf.* 2011.

J.-B. Lagrange[†], J. Pasternak, C. Hunt, V. Blackmore, K. Long
Physics Department, Blackett Laboratory, Imperial College London, Exhibition Road, London, SW7 2AZ, UK
[†] *Also at Fermilab, P.O. Box 500, Batavia, IL 60510-5011, USA*
C. T. Rogers
STFC RAL, UK